ELSEVIER

Journal of Nuclear Materials 271&272 (1999) 326–329

journal of nuclear materials

Observation of spatial distribution of tritium in zirconium alloy with microautoradiography

K. Isobe [a,b,*], Y. Hatano [a], M. Sugisaki [a], T. Hayashi [b], M. Nishi [b], K. Okuno [c]

[a] *Department of Nuclear Engineering, Kyushu University, Fukuoka 812-8581, Japan*
[b] *Japan Atomic Energy Research Institute, Tritium Process Laboratory, Tokai-mura, Naka-gun, Ibaraki-ken 319-1195, Japan*
[c] *Radiochemistry Research Laboratory, Faculty of Science, Shizuoka University, 836 Ohya, Shizuoka 422-8529, Japan*

Abstract

Spatial distribution of tritium in the oxide layer formed on zirconium alloy was examined by tritium microautoradiography. The zirconium alloy (Zircaloy-2) was oxidized in tritiated steam at 673 K. The autoradiographs of the surface and cross-section of the formed oxide films were observed with a scanning electron microscope (SEM). They indicated that the concentration of tritium in the zirconium oxide phase was appreciably high at the oxide surface and decreased sharply with depth. Inside the oxide film, tritium was concentrated in the intermetallic precipitates such as $Zr(Fe,Cr)_2$ and $Zr_2(Fe,Ni)$.

1. Introduction

Tritium autoradiography is an useful experimental technique to examine the spatial distribution of tritium in solid materials. In particular, microautoradiography with a scanning electron microscope (SEM) is a simple and powerful method to obtain microscopic information about the spatial distribution of tritium. Therefore, this experimental technique may be appropriate to study some tritium issues in D–T fusion reactors, e.g. examination of the spatial distribution of tritium in structural materials. The research based on this technique, however, has been sparse, and experimental data are lacking. The usefulness of this experimental technique has not necessarily been widely understood.

Therefore, the objectives of the present study are to accumulate experimental data from tritium microautoradiography and to verify the usefulness of this method to examine the spatial distribution of tritium in metallic materials. In the present work, tritium distribution in zirconium alloys oxidized in tritiated steam has been studied, in particular, attention has been directed to the relation between tritium distribution and the microstructure of the oxide layer since the ingress behavior of tritium into the metallic materials is generally dependent strongly upon the microstructure of oxide film. Although zirconium alloys are not considered as structural materials of D–T fusion reactors, these data may be useful to understand the microscopic mechanism of tritium ingress into structural materials of D–T fusion reactors during oxidation with tritiated water and/or steam at elevated temperatures. The distribution of tritium in the oxide film of zirconium alloys has been examined by Roy [1] and by Cox and Roy [2]. Detailed information about the microstructure of the oxide film, however, was not obtained in their study since they used an optical microscope to observe the autoradiographs [1,2].

2. Experimental

The chemical composition of the zirconium alloy used in the present study is summarized in Table 1. This type of zirconium alloy is called Zircaloy-2 and used as fuel cladding material in boiling water reactors. The disk-type specimens (8.5 mm in diameter and 2 mm in thickness) were annealed in a vacuum at 1073 K for 20 h. The objective of this heat-treatment was to increase the size of intermetallic precipitates such as $Zr_2(Fe,Ni)$

* Corresponding author. Tel.: +81-29 282 6452; fax: +81-29 282 5917; e-mail: isobe@tpl.tokai.jaeri.go.jp

0022-3115/99/$ – see front matter
PII: S0022-3115(98)00694-1

Table 1
Alloy composition of Zircaloy-2 rod

Alloying elements (mass%)				Impurities (mass ppm)		
Sn	Fe	Cr	Ni	O	N	H
1.31	0.18	0.09	0.06	1305	29	8

and $Zr(Fe,Cr)_2$ which are known to be present in Zircaloy-2 as the major precipitates [3]. The specimens were mechanically polished with abrasive paper and finished by polishing with 0.3 μm Al_2O_3 powder.

The microstructure of the specimen was examined by observing the etched surface with a SEM as shown in Fig. 1. The intermetallic precipitates whose average diameter is 0.6 μm were present in the grains and on the grain boundaries.

The experiment was carried out in the Tritium Process Laboratory of Japan Atomic Energy Research Institute. The schematic description of the oxidation apparatus is shown in Fig. 2. This apparatus is placed in the glove box, which is equipped with tritium removal systems. The specimen is suspended from a stainless steel wire inside the tube A. The tritiated water is stored in tube B. The apparatus is evacuated by a turbo-molecular pump.

The specimens were oxidized in tritiated steam for 230 h at 673 K and 0.1 MPa. The procedure of oxidation was the following: The abundance ratio of tritium to hydrogen (T/H) in the steam was 10^{-3}. The tritiated water was frozen by cooling the tube B with dry ice. Next, the apparatus was evacuated. After the pressure inside the apparatus was reduced to less than the detection limit of the gauge, 133 Pa, the valve V_A was closed. Then tritiated water was heated up to 373 K to generate the steam of 0.1 MPa. The specimen was heated up to 673 K. Other parts of apparatus were heated up to above 373 K to prevent the condensation of steam. The specimen was quenched after the oxidation for 230 h by cooling the tube A with water. The tritiated steam was condensed and frozen by cooling the tube B with dry ice. Then the specimen was taken out from the apparatus.

The specimens were ultrasonically cleaned in pure water to remove the tritium adsorbed onto the oxide surface. Here the water was replaced by new one at an interval of 5 min. The radioactivity of tritium in used water was measured after each interval. The counting rate decreased with the duration time of cleaning and became constant after 25 min (the 5 cycles of the replacement); the counting rate was about 1100 dps after the 5 cycles.

The autoradiographs of both surface and cross-section of oxide film were made. In the case of the cross-sectional observation, the specimens were cut with a microsaw in the perpendicular direction to the oxide film. Then the sections were mechanically polished in the manner described above and etched by a solution of nitric and hydrofluoric acid.

The monolayer of the emulsion for autoradiography (Konica NR-H2), in which the average diameter of the AgBr grains was 0.08 μm, was placed on the surface or cross-section of oxide films with a wire-loop method: A loop made of stainless steel wire was dipped in the emulsion diluted by deionized water, and the thin film of the emulsion held in the loop was placed on the specimens by passing the specimens through the loop.

The specimens were kept in a light-tight box filled with helium gas at 77 K to expose the emulsion to the β-ray from tritium. The duration time of exposure was 1 day for the surface observation and 6 days for the cross-

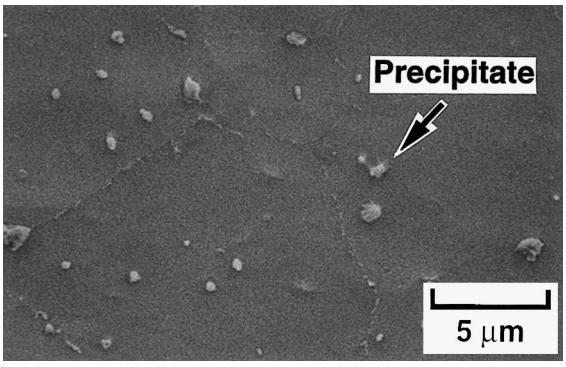

Fig. 1. Microstructure of Zircaloy-2 specimen.

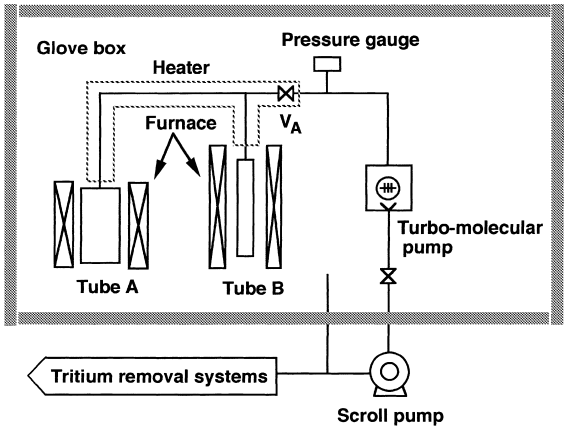

Fig. 2. Schematic description of oxidation apparatus.

sectional observation. Then, the specimens were dipped in a developer solution and then in a fixer solution. The AgBr grains exposed by the β-ray were turned by the development into Ag grains whose average diameter was 0.17 μm. The specimens were dipped in a solution of NaOH (0.01 N) to remove gelatin in the emulsion.

The distribution of Ag grains on the surface or cross-section was observed with the SEM. In the case of surface observation, the specimen was not coated with electrically conductive materials, and hence the charge up of the oxide film was brought about. The degree of charge up is generally different from region to region because the local electronic conductivity of the oxide film is dependent upon the microstructure of oxide. Therefore, we can obtain the information about the microstructure from the difference in brightness in image; the region where the electronic conductivity is high is observed to be dark. The energy of primary electron beam was adjusted to 3 keV in this case because the degree of charge up was high with higher energy and hence the observation was not possible. In the case of cross-sectional observation, the specimen was sputter-coated with Pt–Pd alloy. The energy of primary electron beam was adjusted to 30 keV.

3. Results and discussion

A typical example of autoradiograph of the oxide surface is shown in Fig. 3, in which white spots correspond to the Ag grains. The Ag grains seem to be uniformly distributed on the oxide surface. Dark areas are considered to correspond to the region below which the intermetallic precipitates are present. It is known that the precipitates are embedded in the oxide film in the metallic state [4–8]. Such precipitates in metallic state can act as the expressway of electronic transport through the oxide film and thereby decrease the degree of charge up around them.

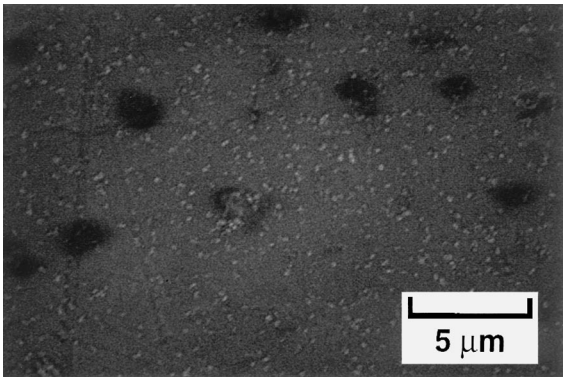

Fig. 3. Tritium microautoradiograph of oxide surface.

The autoradiograph of the cross-section is shown in Fig. 4. In the major part of the cross-section, the Ag grains are uniformly distributed as shown in this figure. The density of Ag grains in the cross-section is low compared with that on the oxide surface (Fig. 3). Many small regions where Ag grains are locally concentrated on like bunches of grapes are present as shown in Fig. 5.

The small regions with high tritium concentration observed in Fig. 5 are considered to be the precipitates embedded in the oxide film since the size of such regions corresponds to that of precipitates. It is well known that the intermetallics of zirconium and 3-d transition metals such as $Zr_2(Fe,Ni)$ and $Zr(Fe,Cr)_2$ have large chemical affinity to hydrogen [9–11]. Since the precipitates remain unoxidized inside the oxide film as mentioned above, tritium is enriched in the precipitates. Such enrichment of tritium was not observed in the study of Roy [1] and Cox and Roy [2] because the precipitates in Zircaloy were too small to be observed with an optical microscope. At the oxide surface, however, such local distribution of tritium is not observed (Fig. 3). This can be attributed to the fact that the precipitates are oxidized at

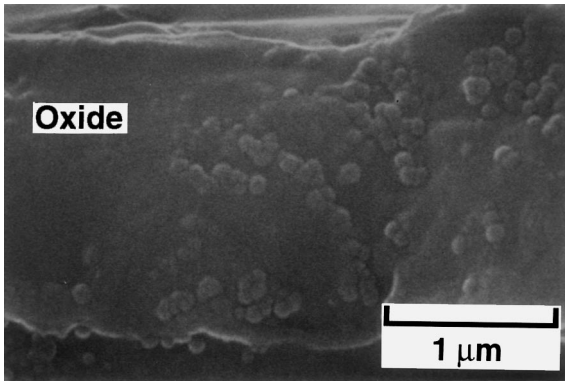

Fig. 4. Tritium microautoradiogarph of cross-section of oxide film.

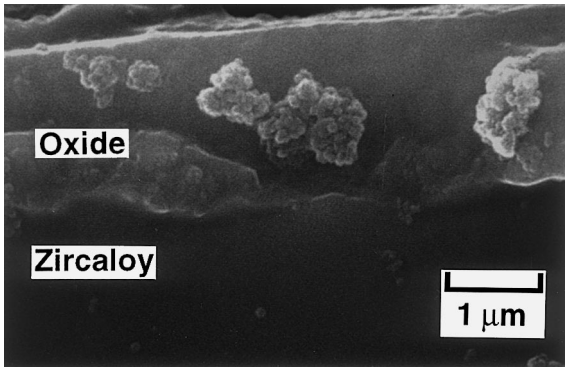

Fig. 5. Tritium microautoradiograph of regions in which tritium was highly concentrated in oxide film.

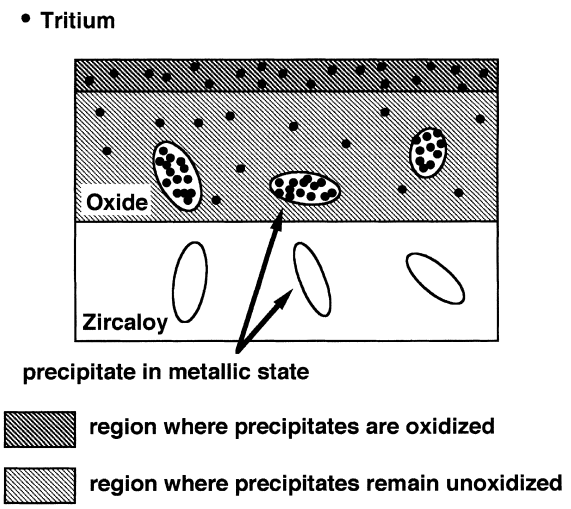

Fig. 6. Schematic description of relation between tritium distribution and microstructure of oxide film.

the oxide surface. The detailed mechanism of oxidation of precipitates at the oxide surface was described in our previous papers [7,8].

The difference in the density of Ag grains between Figs. 3 and 4 indicates that the tritium concentration in the zirconium oxide phase is appreciably high at the oxide surface and sharply decreases with depth. This result is consistent with the depth profile of deuterium in the zirconium oxide phase measured in our previous study [12], in which Zircaloy-2 specimens containing no precipitate observable with the SEM were prepared with heat-treatment and oxidized in D_2O steam. The depth profile of deuterium in the oxide film was measured with secondary ion mass spectroscopy. The deuterium concentration being 0.8 mol% at the oxide surface sharply decreased to 0.2 mol% within the depth of 0.2 μm and gradually decreased in deeper region.

From the above-mentioned results, the schematic description of the relation between the tritium distribution and the microstructure of the oxide film can be given as shown in Fig. 6.

In the previous paper [12], we also examined the influence of size distribution of precipitates on the hydrogen transport through the oxide film and reported that the transport rate was significantly higher for the specimen containing coarse precipitates than for the specimen mentioned above. Therefore, we proposed the model that a large amount of hydrogen is transported through the precipitates. The present result that tritium is concentrated in the precipitates embedded in the oxide film seems to support our model.

4. Conclusions

Spatial distribution of tritium in the oxide layer formed on Zircaloy-2 was examined with microautoradiography. The concentration of tritium in the zirconium oxide phase was appreciably high at the oxide surface and decreased sharply with depth. Inside the oxide film, tritium was concentrated in the intermetallic precipitates such as $Zr(Fe,Cr)_2$ and $Zr_2(Fe,Ni)$.

References

[1] C. Roy, Hydrogen distribution in oxidized zirconium alloys by autoradiography, Atomic Energy of Canada Limited Report AECL-2085, Chalk River Nuclear Laboratories, 1964.
[2] B. Cox, C. Roy, The use of tritium as a tracer in studies of hydrogen uptake by zirconium alloys, Atomic Energy of Canada Limited Report AECL-2519, Chalk River Nuclear Laboratories, 1965.
[3] P. Chemelle, D.B. Knorr, J.B. Van Der Sande, R.M. Pelloux, J. Nucl. Mater. 113 (1983) 58.
[4] T. Kubo, M. Uno, Proceedings of the 9th International Symposium on Zirconium in the Nuclear Industry, Kobe, Japan, 5–8 November 1990, ASTM-STP 1132 (1991) 476.
[5] D. PÍcheur, F. Lefebvre, A.T. Motta, C. Lemaignan, J. Nucl. Mater. 189 (1992) 318.
[6] D. PÍcheur, F. Lefebvre, A.T. Motta, C. Lemaignan, D. Charquet, Proceedings of the 10th International Symposium on Zirconium in the Nuclear Industry, Baltimore, USA, 21–24 June 1993, ASTM-STP 1245 (1994) 687.
[7] Y. Hatano, M. Sugisaki, J. Nucl. Sci. Technol. 33 (1996) 829.
[8] Y. Hatano, M. Sugisaki, J. Nucl. Sci. Technol. 34 (1997) 2648.
[9] D. Shaltiel, I. Jacob, D. Davidov, J. Less-Common Met. 53 (1977) 117.
[10] F. Pourarian, W.E. Wallace, J. Less-Common Met. 107 (1985) 69.
[11] R.M. Van Essen, K.H.J. Buschow, J. Less-Common Met. 64 (1979) 277.
[12] Y. Hatano, K. Isobe, R. Hitaka, M. Sugisaki, J. Nucl. Sci. Technol. 33 (1996) 944.